

Supporting Information

Formation mechanism and photocatalytic activity of hierarchical NiAl-LDH films on Al substrate prepared under acidic conditions

Li Xue,^a Yingzhi Cheng,^{*a,b} Xiuyu Sun,^a Ziyang Zhou,^a Xiaoling Xiao,^b Zhongbo

Hu^b and Xiangfeng Liu^{*b}

^a School of Chemical Engineering, Shandong University of Technology, Zibo

255049, P.R. China.

^b College of Materials Science and Opto-Electronic Technology, University of

Chinese Academy of Sciences, Beijing 100049, P.R. China.

E-mail: chengyz@sdut.edu.cn, liuxf@ucas.ac.cn

1. Materials

All of the reagents used in this work were of analytical grade and used without further purification. The aluminum substrate (purity: 99.99%; thickness: 0.1 mm) was purchased from Xinjiang Joinworld Co., Ltd., China. Ni(NO₃)₂·6H₂O, Zn(NO₃)₂·6H₂O, Co(NO₃)₂·6H₂O and Mg(NO₃)₂·6H₂O were purchased from Sinopharm Chemical Reagent Co., Ltd., Shanghai, China. Ethanol, HNO₃ and NH₃·H₂O were purchased from Laiyang Fine Chemical Factory (China). NaOH and methyl orange (MO) were purchased from Tianjin Bodi Chemical Co., Ltd., China.

1 Rhodamine B (Rh B) was obtained from Aladdin Reagent Co., Ltd., Shanghai, China.

2 Deionized water was used in all the experimental processes.

3 **2. Preparation of NiAl-LDH/Al films**

4 The NiAl-LDH film was prepared by a simplified *in situ* growth technique. The
5 aluminum sheet (2×3 cm) was cleaned with ethanol, 1 M NaOH solution and
6 deionized water in sequence before use. The 0.1 M Ni²⁺-containing solution was
7 obtained by dissolution of Ni(NO₃)₂·6H₂O in deionized water, and the pH value was
8 adjusted to 1, 2, 3, 4, 5 and 6 respectively, by addition of NH₃·H₂O or HNO₃. Each
9 resulting solution was transferred to a glass tube, and the as-prepared Al substrate was
10 placed vertically in the solution. The tube was sealed by cling film and heated to 80
11 °C in water bath for different times. The pH values of the solutions were detected at
12 regular time intervals at room temperature. The resulting films were rinsed with
13 deionized water and dried under ambient conditions. The precipitate in bulk solution
14 was filtrated, washed with deionized water and dried under ambient conditions. The
15 white film coating on Al substrate is denoted as NiAlp_xt_y, and the precipitate formed in
16 bulk solution is denoted as NiAlp_xt_y-p (*x* means the initial pH value of the
17 Ni²⁺-containing solution and *y* means the immersion time (hour) of the Al substrate in
18 solution).

19 Solutions containing Zn²⁺, Co²⁺ and Mg²⁺ respectively were prepared to fabricate
20 MAlp₂t₂₄ (M=Zn, Co, Mg) samples, using the same *in situ* growth method as

1 NiAlp2t24.

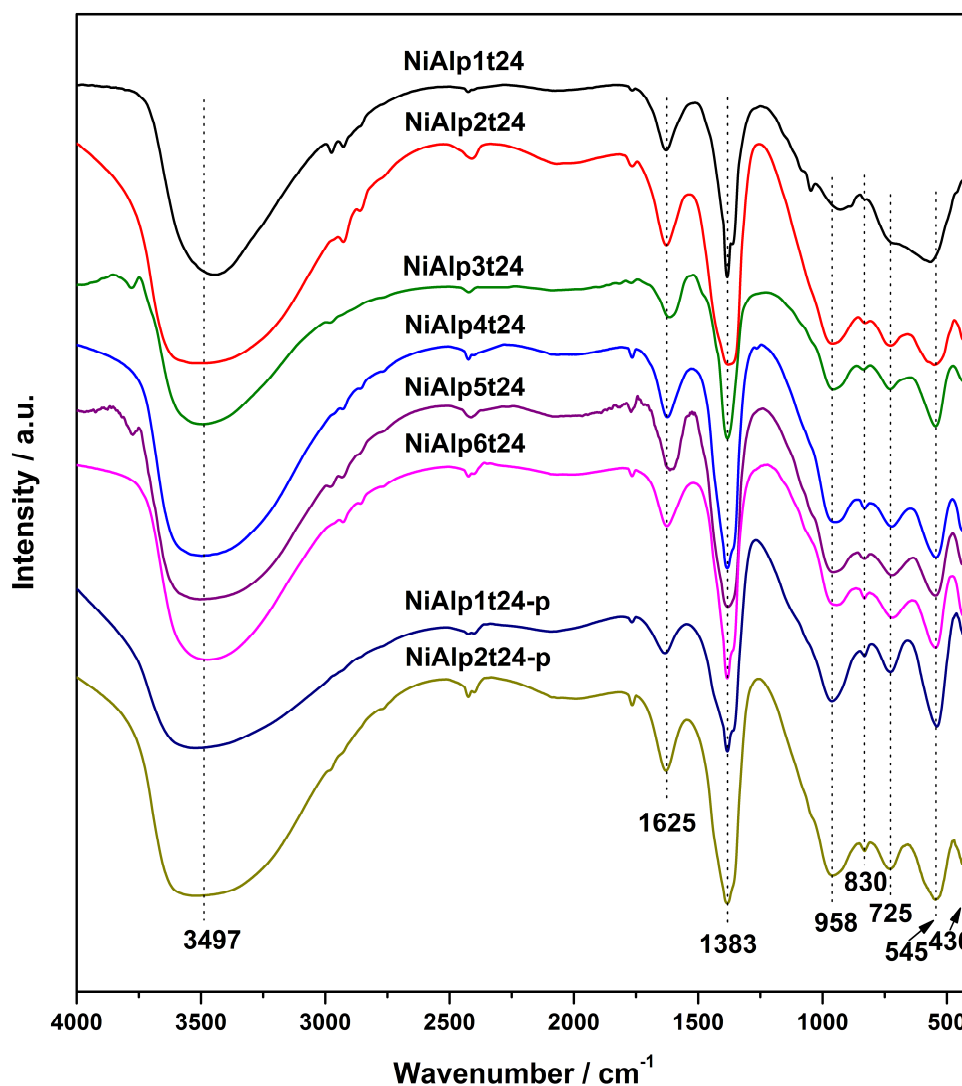
2 **3. Sample Characterization**

3 The powder X-ray diffraction (XRD) measurements were performed on a Bruker
4 D8 Advance X-ray diffractometer (Cu K α radiation, $\lambda = 1.5406 \text{ \AA}$) at 35 kV, 30 mA,
5 with a scan step of 0.02° and a 2θ angle ranging from 5° to 70° . Fourier transform
6 infrared (FT-IR) spectra of samples were collected in KBr pellets on a Nicolet 5700
7 Fourier transformation infrared spectroscope (Thermo Electron Co., USA), at the
8 range of $400\text{-}4000 \text{ cm}^{-1}$ with a resolution of 4 cm^{-1} . The morphology of the samples
9 was investigated using a field emission scanning electron microscope (FESEM, FEI
10 Sirion 200, Netherlands) with an energy-dispersed X-ray (EDX) unit (INCA Oxford).
11 The accelerating voltage applied was 10 kV. All samples were sputtered with platinum.
12 To investigate the surface nature of samples, X-ray photoelectron spectroscopy (XPS)
13 spectra were recorded on an ESCALAB 250Xi X-ray photoelectron spectrometer
14 using Al K α radiation with constant pass energy of 20 eV.

15 The photocatalytic activity of the film samples was evaluated by photocatalytic
16 degradation of MO and Rh B in aqueous solution. In the case of MO degradation, a 50
17 mL of 20 mg L^{-1} MO was placed in a photocatalytic reactor, to which a film catalyst
18 ($2 \times 3 \text{ cm}$) was added lying on the bottom of the reactor. Then the solution was
19 irradiated immediately with ultraviolet light from a high-pressure mercury lamp (125
20 W, GGZ-125, Shanghai Yaming Fiya Lighting Appliance Co., Ltd., $E_{\text{max}} = 365 \text{ nm}$)

1 under stirring condition without preadsorption of MO on catalyst. Although the LDH
2 film covers both side of the Al substrate, only one side of the film sample was
3 exposed to the mercury lamp which was located above the reactor. As for Degussa
4 P25 TiO₂, 1.0 mg TiO₂ was added into the MO solution for the photodegradation
5 reaction. The weight of the TiO₂ was equal to the weight of LDH powder scraped
6 from two sides of one Al substrate (NiAlp2t24 sample). The temperature of the
7 solution was controlled at room temperature by circulating water. During irradiation,
8 at given time intervals, the concentration of MO was monitored by colorimetry using
9 a UV/VIS spectrophotometer (UV-1801, Beijing Beifen-Ruili Analytical Instrument
10 (Group) Co., Ltd.). Centrifugation was performed to separate the TiO₂ powder from
11 the solution to determine the concentration of MO when P25 TiO₂ was used as
12 photocatalyst. Blank dye degradation was also carried out under similar condition
13 without the catalyst. MO adsorption experiments on NiAlp_xt₂₄ ($x = 1-6$) were
14 performed under stirring condition in the dark. In the case of photodegradation of Rh
15 B, a 50 mL of 50 mg L⁻¹ Rh B solution was used for NiAlp2t24 and P25 TiO₂
16 photocatalysts.

1 4. Characterization and Results

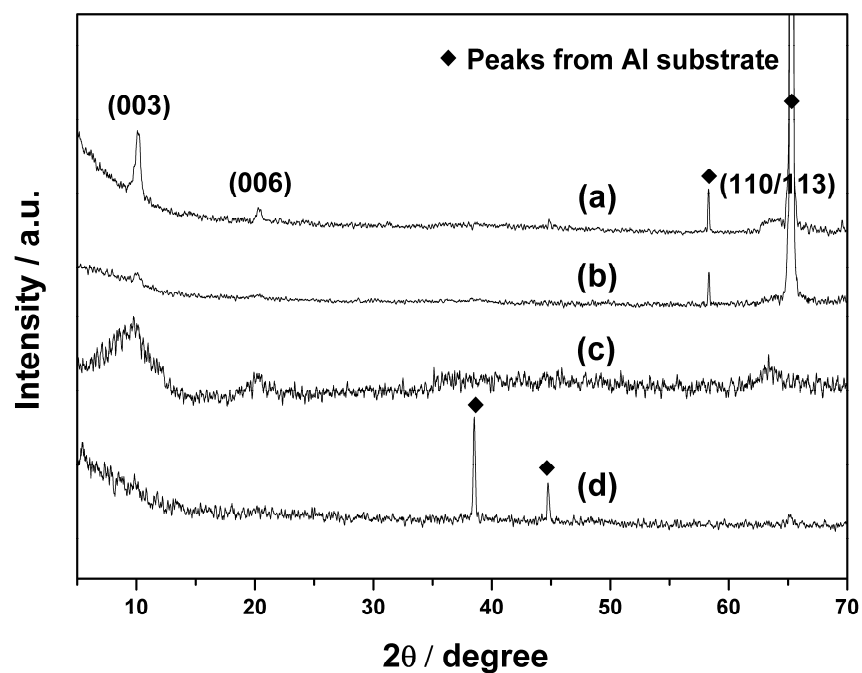


2

3 Fig. S1 FT-IR spectra of scraped powder of NiAlp_xt₂₄ ($x = 1-6$) and NiAlp_xt₂₄-p ($x =$
4 1, 2).

5 The broad and intense band centered around 3497 cm^{-1} is due to the OH stretching
6 mode of layer hydroxyl groups and of interlayer water molecules.¹⁻³ All samples have
7 a weak peak centered at 1625 cm^{-1} . This peak is associated with the bending mode of
8 water.¹⁻³ The intense band at 1383 cm^{-1} and weak band at 830 cm^{-1} are ascribable to

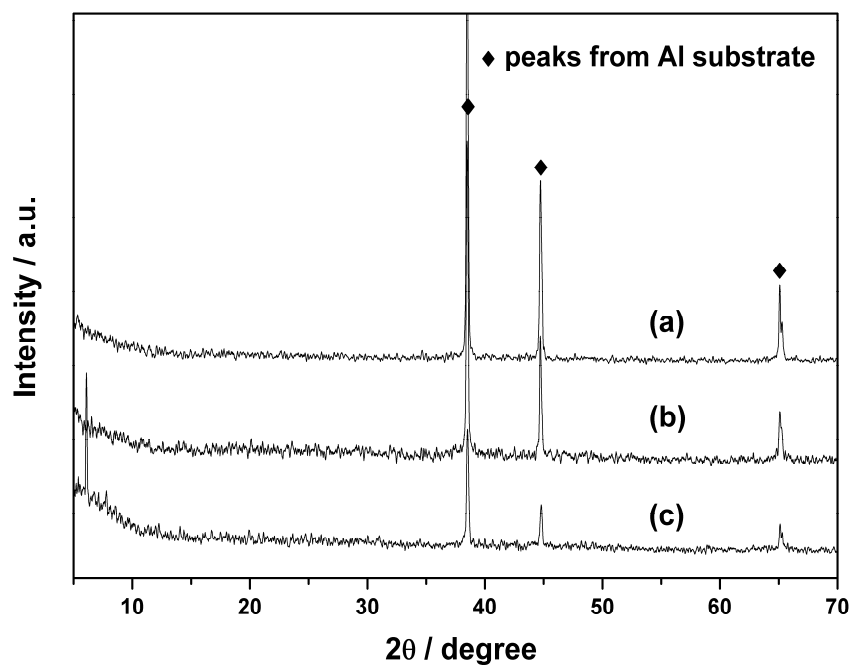
1 the stretching and the bending mode of the nitrate anions respectively ^{2,3}, suggesting
2 that NO₃⁻ is the intercalated anion of NiAl-LDH in NiAlp_xt₂₄ ($x = 2-6$) and
3 NiAlp_xt₂₄-p ($x = 1, 2$). The bands around 725 and 545 cm⁻¹ can assigned to
4 translation modes of the hydroxyl groups influenced by Al³⁺.^{1,4} The corresponding
5 deformation mode is observed at around 958 cm⁻¹.^{1,4} According to the literatures, the
6 band centered at 430 cm⁻¹ can be ascribed to M-O-M bonds ³ or translation modes of
7 the hydroxyl groups influenced by Al³⁺.¹ The FT-IR spectra of NiAlp_xt₂₄ ($x = 2-6$)
8 and NiAlp_xt₂₄-p ($x = 1, 2$) are very similar to each other due to the same LDH
9 structure. The spectrum of NiAlp₁t₂₄, however, is quite similar to the spectrum of
10 amorphous aluminum hydroxide reported in ref. 5, showing different features from
11 those of NiAlp_xt₂₄ ($x = 2-6$) in the wavelength range of 1000-400 cm⁻¹.



1

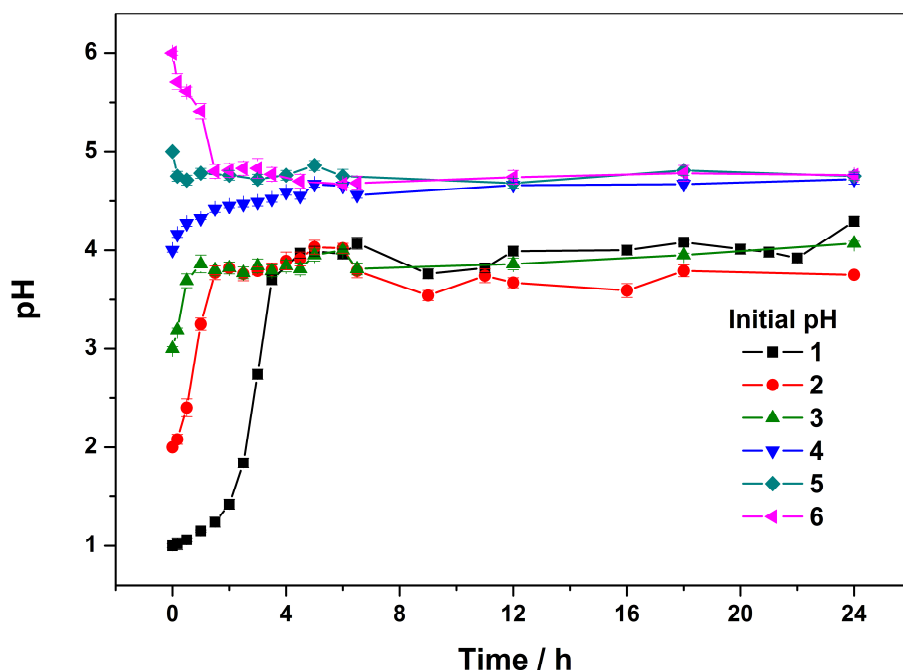
2 Fig. S2 XRD patterns of (a) NiAlp2t72 film, (b) NiAlp2t24 film, (c) NiAlp2t12-p and

3 (d) scraped powder of NiAlp2t12 film.



1

2 Fig. S3 XRD patterns of scraped powders of (a) ZnAlp2t24, (b) CoAlp2t24 and (c)
3 MgAlp2t24. Diffraction peaks of LDHs were not detected in the XRD patterns of the
4 three samples.



1

2 Fig. S4 Variations of pH value of Ni^{2+} -containing solution during the immersion of Al
3 substrates in it.

4 Figure S4 plots pH curves of Ni^{2+} -containing solutions against reaction time.

5 According to the final pH value, these curves can be roughly divided into two groups:

6 solutions with initial pH 1-3 experienced increase of pH value to 3.7-4.3, and

7 solutions with initial pH 4-6 experienced increase or decrease of pH value to 4.7-4.8.

8 The increase of the solution pH value can be attributed to the consumption of H^+ by

9 reacting with aluminium, providing Al^{3+} . At the same time, tiny bubbles were

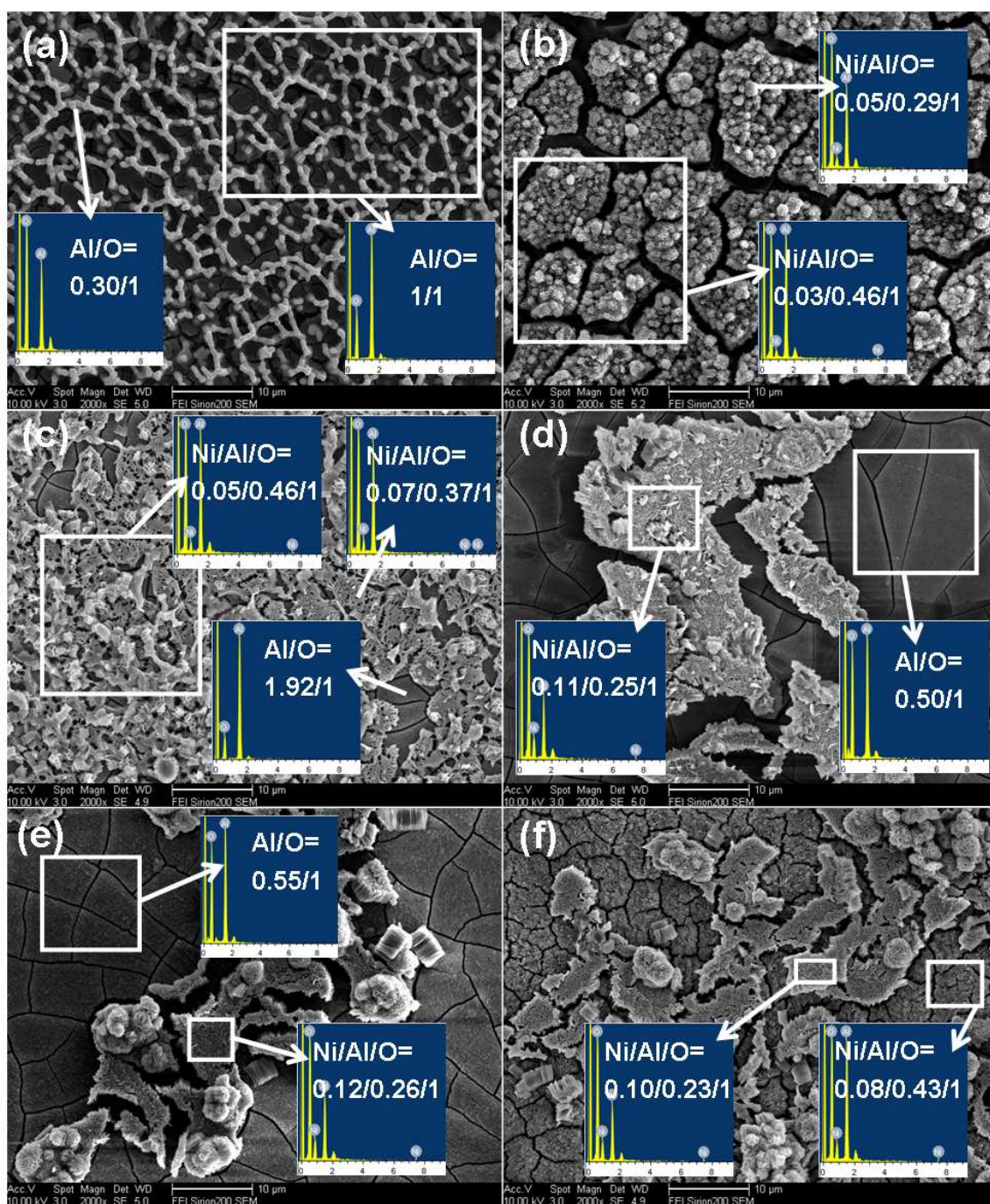
10 observed forming on the surface of Al substrate during the reaction. The lower the

11 initial pH value, the higher the concentration of Al^{3+} in solution. The high

12 concentration of Al^{3+} is supposed to be responsible for the formation of LDH

13 precipitation in bulk solutions with initial pH 1 and 2.

1 In addition, it has been reported that aluminium can dissolve at the interface by
2 reacting with OH^- to form $\text{Al}(\text{OH})_3$ or $\text{Al}(\text{OH})_4^-$ species in alkaline condition (at pH
3 7-8).⁶ In this work, although the reaction was carried out in acidic condition, the rapid
4 decrease of the pH value of solutions with initial pH 5 and 6 suggests that similar
5 reactions may occur, i.e., aluminium hydr(ous) oxide species began to form soon after
6 the Al substrates were immersed into the corresponding solutions.

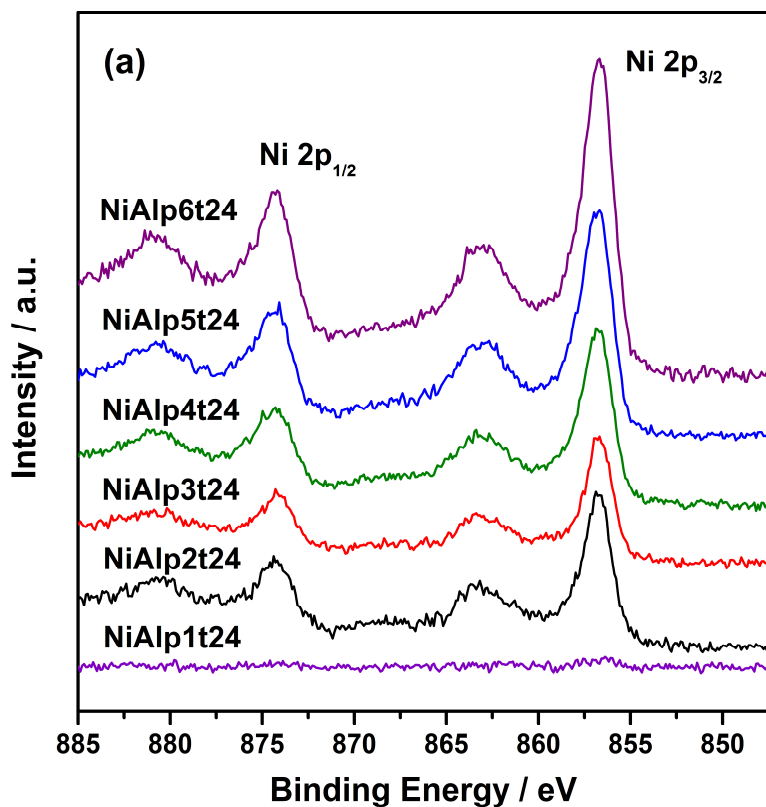


1

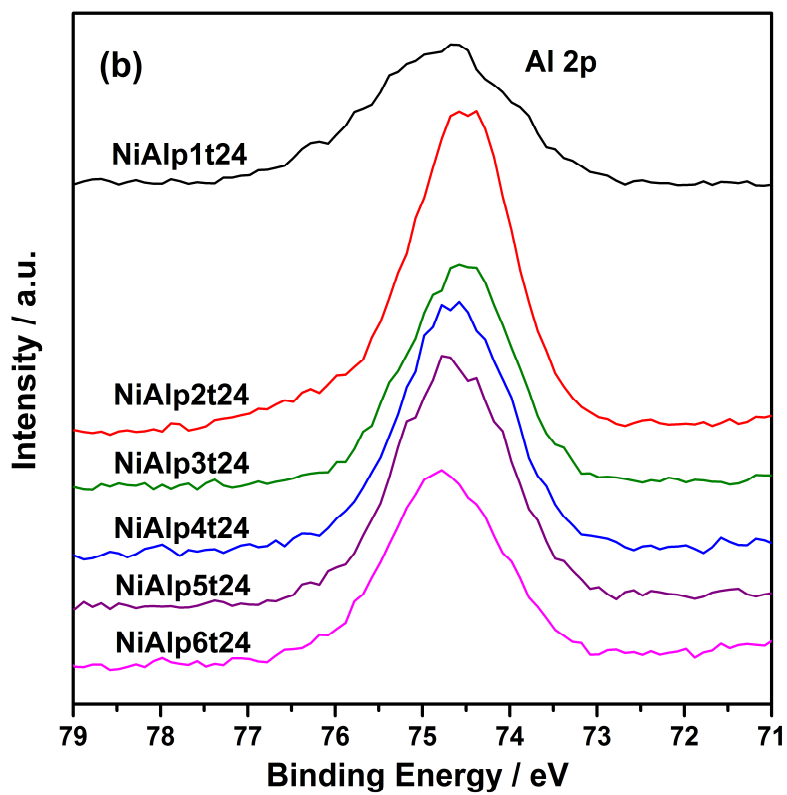
2 Fig. S5 SEM images of NiAlp_xt₂₄, x = (a) 1, (b) 2, (c) 3, (d) 4, (e) 5 and (f) 6. Insets are
3 the EDX results of corresponding areas and spots.

4 According to Fig. S5, signal of Ni has not been detected on NiAlp₁t₂₄ and those
5 pillar-like protrusions should be amorphous aluminium hydroxide which is consistent
6 with the FT-IR result (Fig. S1) and the XRD result (Fig. 1). As the initial pH value of

1 Ni²⁺-containing solution increasing from 2 to 6, the Ni/Al ratio of NiAl_px_t24 ($x = 2, 3,$
2 4, 5, 6) LDH film increased simultaneously. At the same time, an interlayer of
3 aluminium hydr(ous) oxide can be observed between the LDH film and Al substrate
4 on NiAl_px_t24 ($x = 3, 4, 5$) with the peeling of LDH film. And a new layer of
5 microcrystal began to form on the exposed interlayer on NiAl_p6_t24.



1

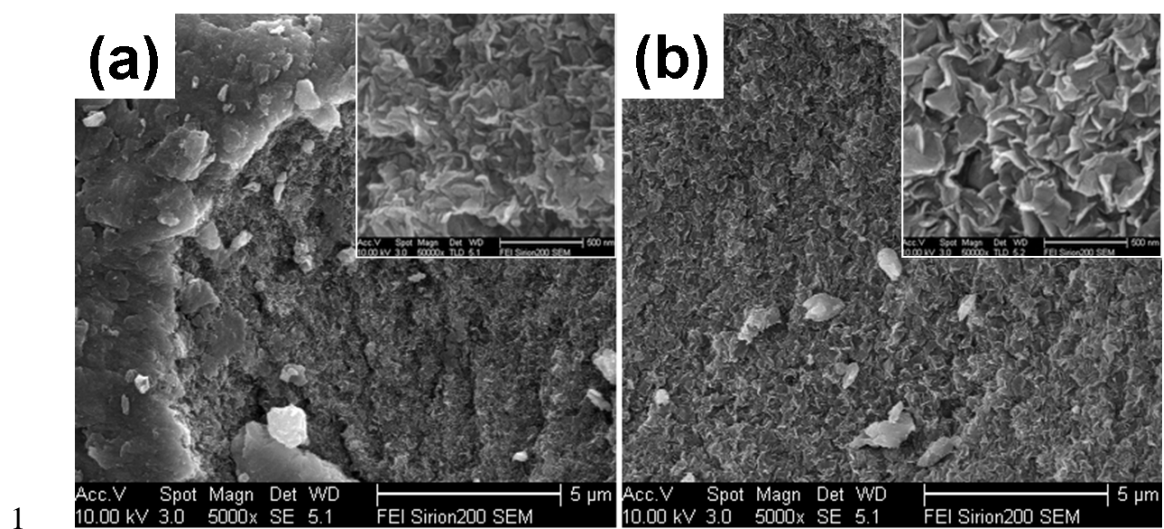


2

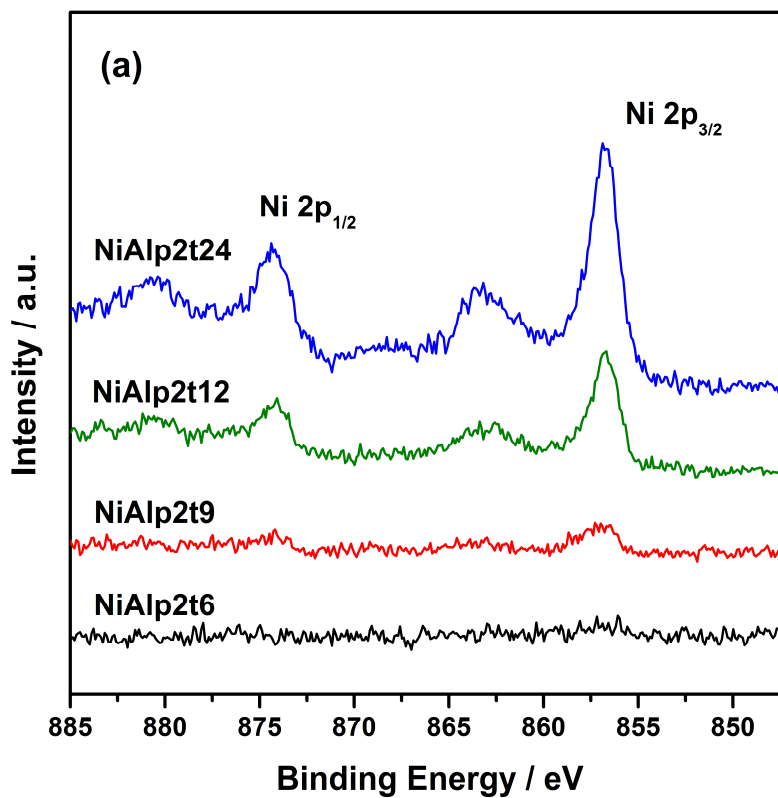
3 Fig. S6 XPS spectra of NiAlp_xt₂₄ (x = 1-6) films, (a) Ni 2p and (b) Al 2p.

1 From Fig. S6 (a), it can be seen that the binding energy (BE) values of the main Ni
2 $2p_{3/2}$ peak are approximately in the same region (around 856.7 eV), suggesting that
3 the electronic state of Ni in NiAlp x t 24 ($x = 2-6$) are similar. Signal of Ni was not
4 detected in NiAlp1t 24 , which is consistent with the EDX result presented in Fig. S5.

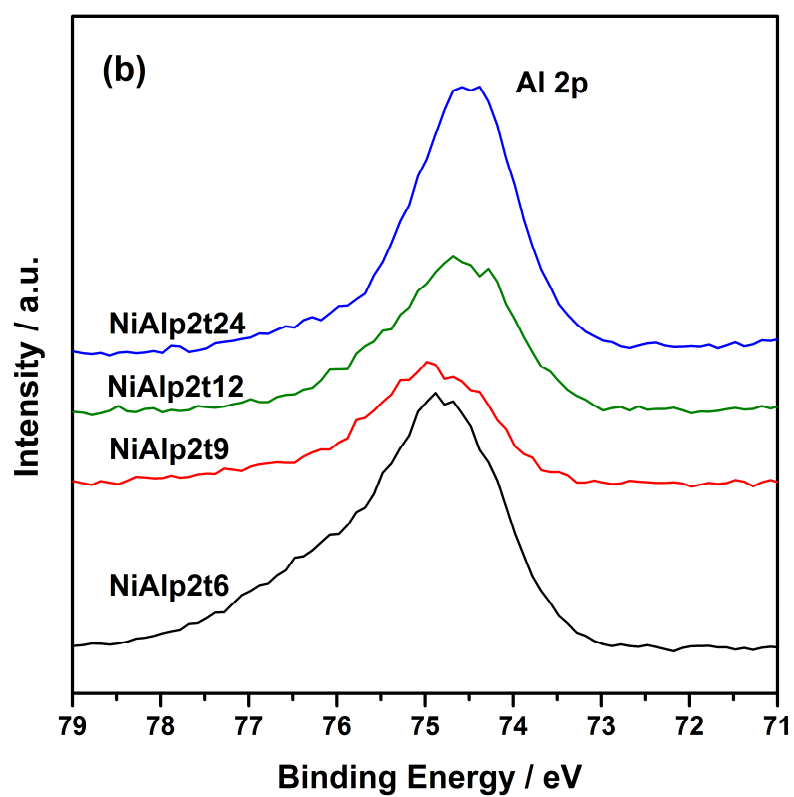
5 The Al 2p BE values of NiAlp x t 24 are in the range of 74.29 eV \sim 74.79 eV,
6 implying the difference of chemical environment of Al. The broad Al 2p peak of
7 NiAlp1t 24 centred at 74.68 eV is assigned to the Al³⁺ in aluminium hydr(ous) oxide.
8 When the NiAl-LDH phase was formed, the Al 2p peak (NiAlp2t 24) shifted to a
9 lower value by 0.4 eV (around 74.29 eV). Similar variation of Al 2p BE value during
10 the formation of the LDH phase was also reported by Y. Yang et al.⁵ and Y. F. Gao et
11 al..⁷ Consulting the references, we suggest that formation of the Al-O-Ni bond in
12 NiAl-LDH leads to increase in charge density of outer orbital of Al and decrease in
13 binding energy compared to the Al-O-Al bond in aluminium hydr(ous) oxide. With
14 the increase of the initial pH value (pH = 3-6), the peeling of the LDH film became
15 severer. The BE value of Al 2p shifted back to higher value due to the exposure of
16 aluminium hydr(ous) oxide interlayer on NiAlp x t 24 ($x = 3-6$).



1
2 Fig. S7 SEM images of (a) NiAlp1t24-p and (b) NiAlp2t24-p. Insets are images at
3 high magnification.



1

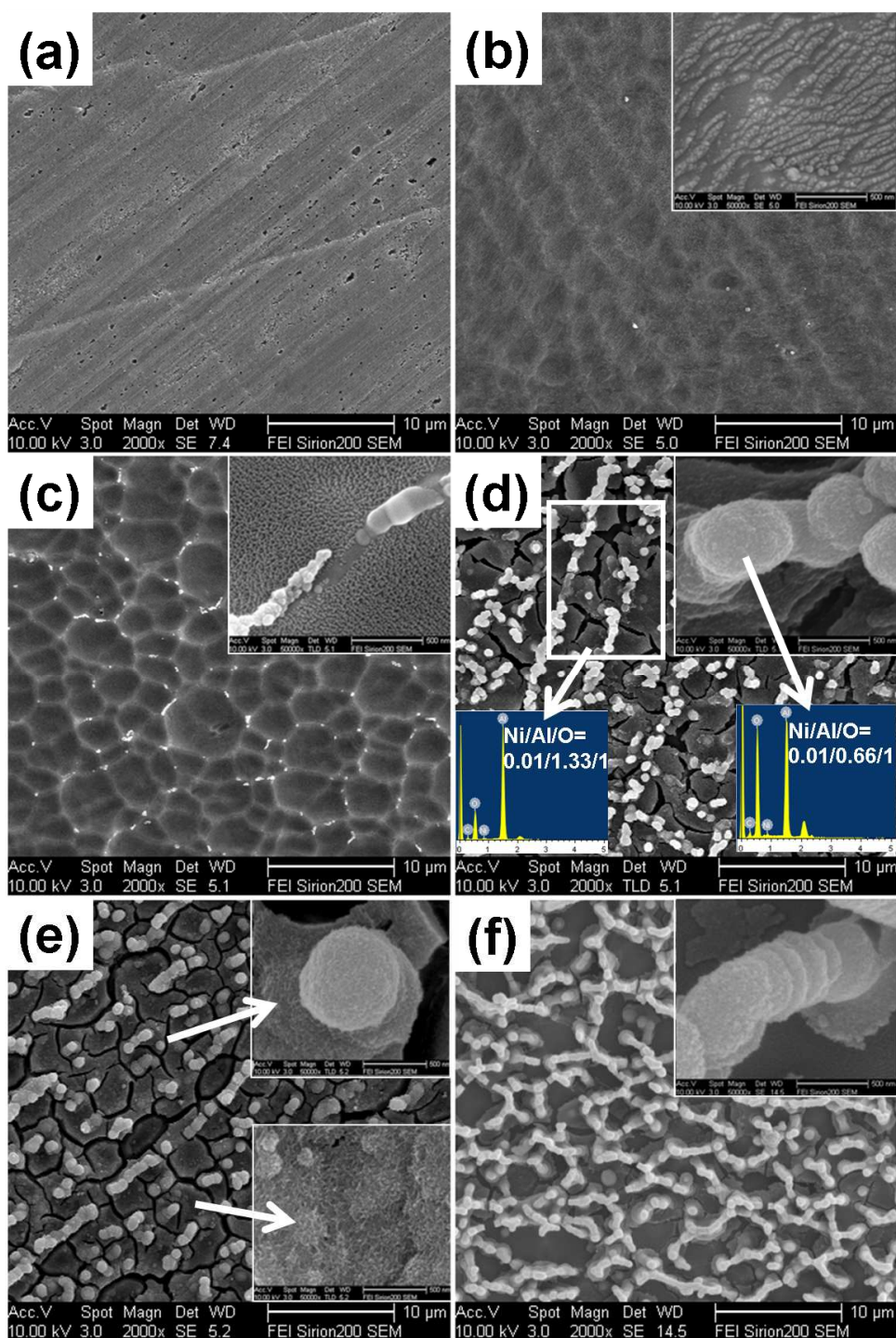


2

3 Fig. S8 XPS spectra of NiAlp2ty films ($y = 6, 9, 12, 24$), (a) Ni 2p and (b) Al 2p.

1 XPS measurements have been performed to investigate the surface nature of
2 NiAlp2ty. From the spectra of Ni 2p presented in Fig. S8(a), it can be seen that the BE
3 value of Ni 2p_{3/2} (NiAlp2ty, y = 9, 12, 24) are approximately in the same region
4 (around 856.8 eV) except for NiAlp2t6, suggesting that the electronic states of Ni are
5 similar. This result implies that the Ni²⁺ was not involved in the NiAl-LDH formation
6 reaction until 9 h later.

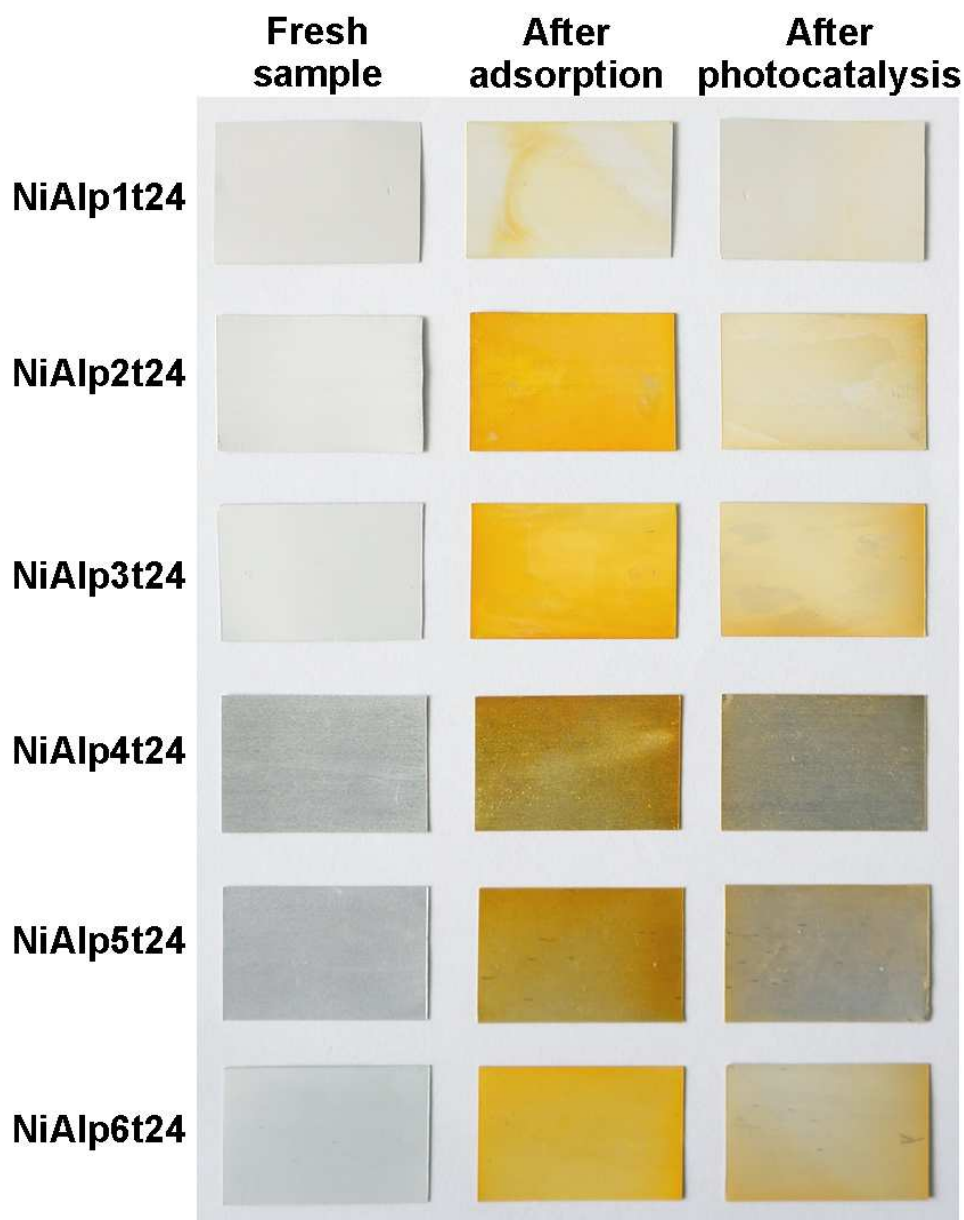
7 According to the XPS spectra of Al 2p shown in Fig. S8(b), the shift of the Al 2p
8 BE to lower values with increasing reaction time from 6 to 24 h is obvious. This result
9 indicates that the electronic atmosphere of Al atom was changed. The formation of
10 Al-O-Ni bond in NiAl-LDH on aluminium hydr(ous) oxide interlayer must be
11 responsible for the negative shift in Al 2p BE value.²



1

2 Fig. S9 SEM images of surface morphology of Al substrate immersed in
3 Ni^{2+} -containing solution with initial pH 1 for (a) 0 h, (b) 6 h, (c) 12 h, (d) 16 h, (e) 20
4 h and (f) 24 h at low magnification. Insets are images at high magnification and the
5 EDX results of corresponding area and spot.

1 Although the evolution of solution's pH value of NiAlp1t24 exhibits a similar trend
2 with that of NiAlp2t24, the SEM images of NiAlp1t24 shown in Fig. S9 are not just
3 replications of NiAlp2t24 at similar pH values. After 6 h reaction, the Al substrate
4 was covered with shallow pits, 2-4 μm in diameter, as a result of the corrosion by acid.
5 Stripes formed by tiny spots can be observed in the inset (Fig. S9(b)). The pits
6 became deeper with white protrusions formed on the edges after 12 h (Fig. S9(c)).
7 When the reaction time increased to 16 h, numerous white pillar-like protrusions were
8 formed on the network-like cracked substrate. The composition of the protrusions by
9 EDX is Ni/Al/O=0.01/0.66/1. This result suggests that alumina has been formed on
10 the substrate, which is different from the AlOOH on NiAlp2t6 (Al/O=0.51/1, Fig. 3).
11 After a prolonged reaction time of 20 h, a layer of microcrystal began to form, which
12 can be observed in Fig. S9(e). However, LDH platelets were not observed in Fig.
13 S9(f). Formation of Al(OH)₃ on NiAlp1t24 was confirmed by EDX (Fig. S5) and
14 FT-IR (Fig. S1) results, which indicates that these microcrystals (Fig. S9(e)) are not
15 nuclei of LDH crystallite. In fact, the Al₂O₃ on NiAlp1t16 converted to Al(OH)₃ (Fig.
16 S5(a)) when the immersion time extended to 24 h. Based on the above observation,
17 we conclude that LDH could not be formed on the phase boundary of Al₂O₃ at present
18 condition. The formation of aluminium hydr(ous) oxide interlayer may be the main
19 factor which resulting in the formation of LDH crystallites on NiAlp_xt₂₄ ($x = 2-6$).

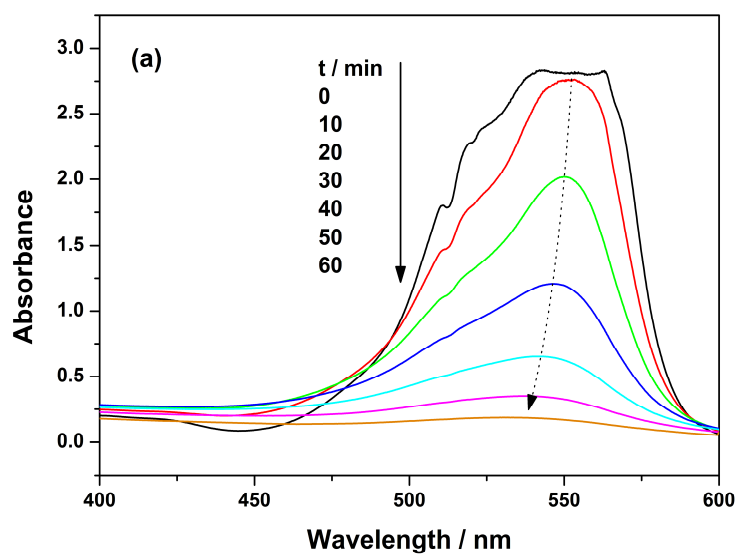


1

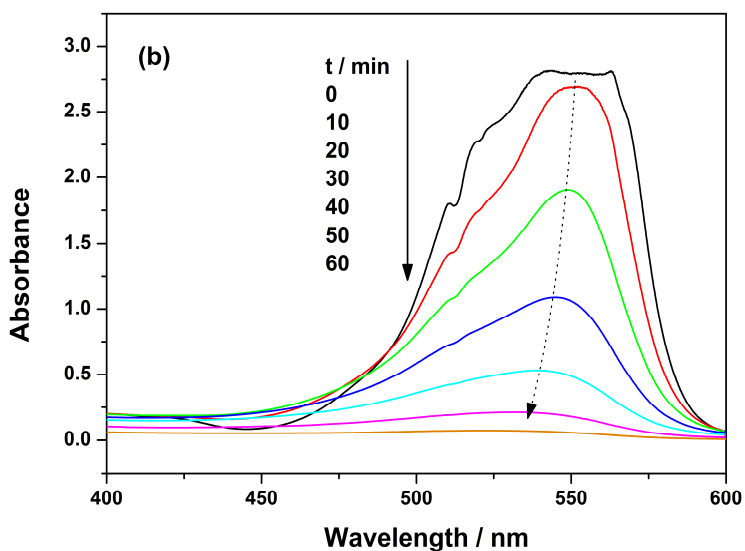
2 Fig. S10 Digital photograph of fresh NiAlp_xt₂₄ samples, samples after MO adsorption
3 experiments and samples after MO photocatalysis experiments.

4 From Fig. S10, it is clear to see that compared to fresh samples, NiAlp_xt₂₄ turned
5 yellow after the adsorption experiments, suggesting the adsorption of MO on the
6 sample surface. Meanwhile, the colors of samples after photocatalysis experiments are
7 much lighter than those after adsorption experiments, although experimental

1 conditions are identical except for the UV irradiation in the photocatalysis
2 experiments. This distinct difference in color indicates that MO adsorption on
3 NiAlp_{xt}24 has little effect on the MO concentration during the photocatalytic reaction.
4 The decrease of the MO concentration should be mainly ascribed to photocatalysis of
5 NiAlp_{xt}24 other than MO adsorption on NiAlp_{xt}24 under UV irradiation.



1



2

3 Fig. S11 Spectral changes of Rh B (initial concentration 50 mg L⁻¹) over the catalysts,
4 (a) NiAlp2t24 and (b) P25 TiO₂.

5 As shown in Fig. S11, the absorption maximum of the Rh B solution steadily
6 decreases with increasing irradiation time, indicating gradual degradation of the Rh B.
7 The photocatalytic performance of NiAlp2t24 LDH film is similar to that of P25 TiO₂
8 powder in photodegradation of Rh B.

1 **References:**

- 2 1. J. T. Kloprogge, L. Hickey and R. L. Frost, *J. Solid State Chem.*, 2004, **177**, 4047.
- 3 2. K. Li, N. Kumada, Y. Yonesaki, T. Takei, N. Kinomura, H. Wang and C. Wang,
4 *Mater. Chem. Phys.*, 2010, **121**, 223.
- 5 3. E. Scavetta, B. Ballarin, C. Corticelli, I. Gualandi, D. Tonelli, V. Prevot, C. Forano
6 and C. Mousty, *J. Power Sources*, 2012, **201**, 360.
- 7 4. J. T. Kloprogge and R. L. Frost, *J. Solid State Chem.*, 1999, **146**, 506.
- 8 5. Y. Yang, X. Zhao, Y. Zhu and F. Zhang, *Chem. Mater.*, 2012, **24**, 81.
- 9 6. K. Dutta, S. Das, A. Pramanik, *J. Colloid. Interf. Sci.*, 2012, **366**, 28.
- 10 7. Y. F. Gao, M. Nagai, Y. Masuda, F. Sato, W. S. Seo and K. Koumoto, *Langmuir*,
11 2006, **22**, 3521.